

Exact Solitonic Solutions of the Gross-Pitaevskii Equation with a Linear Potential

Usama Al Khawaja

Physics Department, United Arab Emirates University,
P.O. Box 17551, Al-Ain, United Arab Emirates.

(Dated: September 13, 2021)

We derive classes of exact solitonic solutions of the time-dependent Gross-Pitaevskii equation with repulsive and attractive interatomic interactions. The solutions correspond to a string of bright solitons with phase difference between adjacent solitons equal to π . While the relative phase, width, and distance between adjacent solitons turn out to be a constant of the motion, the center of mass of the string moves with a constant acceleration arising from the inhomogeneity of the background.

PACS numbers:

Introduction—The experimental realization of dark solitons [1, 2, 3], bright solitons [4, 5], and recently gap solitons [6] in Bose-Einstein condensates has stimulated intense interest in their properties particularly their formation and propagation [7, 8, 9, 15, 16, 17]. Due to the nonlinearity arising from the interatomic interactions and due to the presence of a confining potential in the Gross-Pitaevskii equation that describes the evolution of the solitons, these studies were performed either by solving the corresponding Gross-Pitaevskii equation numerically or by using perturbative methods. Interestingly enough, some exact solitonic solutions were recently found for this equation in one dimension, but with time- and space-dependent interatomic interactions and trapping potential strengths [10, 11, 12, 13, 14]. Obtaining such exact solutions allows for testing the validity of the Gross-Pitaevskii equation at high densities, obtain the long-time evolution of the soliton where numerical techniques may fail, and helps to understand soliton formation and propagation.

The so-called Darboux transformation method [18] was used to obtain such exact solutions. We have shown in a previous work [19] that such exact solutions may exist only for specific functional forms for the interatomic interaction and trapping potential strengths. For example, in the work of Liang *et al.* [12], the exact solution is found only when the trapping potential is quadratic, repulsive, and the interatomic interaction strength is growing exponentially with time with a rate that equals the trapping potential strength itself. Such a restriction, makes the exact solution less interesting from an experimental point of view. In an attempt to soften this restriction, we found that exact solutions may also be found for constant, linear, or quadratic potentials, and with interatomic interaction strengths that can be constant, growing, or decaying in time [19].

Here, we exploit our previous result to obtain exact solitonic solutions of the time-dependent Gross-Pitaevskii equation with linear trapping potential and constant interatomic interaction strength that can be positive or negative. The Gross-Pitaevskii equation de-

scribes, in this case, the surface of the condensate.

The Gross-Pitaevskii equation.—Near the surface of a Bose-Einstein condensate, the quadratic trapping potential can be approximated by a linear potential and the surface of the condensate can be regarded as an infinite plane. The Gross-Pitaevskii equation, in this case, takes the form [22, 23]

$$i\hbar \frac{\partial \psi(x, t)}{\partial t} = \left[-\frac{\hbar^2}{2m} \frac{\partial^2}{\partial x^2} + Fx + \frac{4\pi a \hbar^2}{m} |\psi(x, t)|^2 \right] \psi(x, t), \quad (1)$$

where $\psi(x, t)$ is the condensate wavefunction, and x is the coordinate normal to the surface of the condensate such that the bulk of the condensate exists in the region $x < 0$. The force constant F arises from linearizing the harmonic potential near the surface, namely $F = m\omega^2 R$, where ω is the characteristic frequency of a spherically symmetric harmonic trapping potential, R is the radius of the condensate, and m is the mass of an atom. The interatomic interaction strength is proportional to the scattering length a which can be positive or negative.

The characteristic length δ in the surface region is defined by equating the kinetic energy $\hbar^2/2m\delta^2$ to the potential energy $F\delta$, namely $\delta = (\hbar^2/2mF)^{1/3}$. Scaling length to δ , time to $\tau = 2m\delta^2/\hbar$, and the wavefunction to $\sqrt{\rho_0} = 1/\sqrt{8\pi|a|\delta^2}$, the previous equation takes the dimensionless form

$$i \frac{\partial \psi(x, t)}{\partial t} = \left[-\frac{\partial^2}{\partial x^2} + x - p^2 |\psi(x, t)|^2 \right] \psi(x, t), \quad (2)$$

where we have retained the nonscaled symbols for convenience. The parameter $p^2 = -\text{sgn}(a)$ allows for treating the repulsive case ($p^2 = -1$) and attractive case ($p^2 = 1$) simultaneously.

For the case of repulsive interactions, the Thomas-Fermi approximation can be used to estimate δ and ρ_0 in terms of the size of the condensate, R , and the central density ρ_{TF} [20]. It turns out that $\delta/R \approx \gamma^{-4/15}$ and $\rho_0/\rho_{\text{TF}} \approx \gamma^{-4/15}$, where $\gamma = Na/a_0$ is the dimensionless interaction strength, $a_0 = \sqrt{\hbar/m\omega}$ is the characteristic length of the harmonic oscillator potential, and N is the

number of atoms. For a typical ^{87}Rb condensate with 10^4 atoms the two ratios are roughly equal to $1/4$. The unit of time is, in this case, given by $\tau \approx 2\gamma^{-1/15}/\omega$. Approximating the quadratic potential of the Bose-Einstein condensate by a linear one in the surface region is accurate only within a region of width δ around the *Thomas-Fermi* surface. It turns out, however, that some of the solitonic solutions we obtain here have width larger than δ . Furthermore, the dynamics of these solitons is such that they drift from the surface region towards the bulk region of the condensate where the potential is not linear anymore. Therefore, such solutions can be considered only as the initial states of the time-dependent solitonic excitations of the condensate.

The Darboux Transformation and the New Solutions.— The first step in the Darboux transformation method is to find a linear system of equations for an auxiliary field $\Psi(x, t)$ such that Eq. (2) is its consistency condition [18]. Using the method described in Ref. [19], we find that the following linear system corresponds to Eq. (2)

$$\Psi_x = \mathbf{J}\Psi\Lambda + \mathbf{U}\Psi, \quad (3)$$

$$i\Psi_t = \mathbf{W}\Psi + 2(\zeta\mathbf{J} + \mathbf{U})\Psi\Lambda + 2\mathbf{J}\Psi\Lambda^2, \quad (4)$$

$$\text{where, } \Psi(x, t) = \begin{pmatrix} \psi_1(x, t) & \psi_2(x, t) \\ \phi_1(x, t) & \phi_2(x, t) \end{pmatrix}, \quad \mathbf{J} = \begin{pmatrix} 1 & 0 \\ 0 & -1 \end{pmatrix}, \quad \Lambda = \begin{pmatrix} \lambda_1 & 0 \\ 0 & \lambda_2 \end{pmatrix}, \quad \mathbf{U} =$$

$$\begin{pmatrix} \zeta & pq(x, t)/\sqrt{2} \\ -pr(x, t)/\sqrt{2} & -\zeta \end{pmatrix},$$

$\mathbf{W} = (\zeta^2 - x/2)\mathbf{J} + 2\zeta\mathbf{U} - \mathbf{J}(\mathbf{U}^2 - \mathbf{U}_x)$, $\zeta(t) = it/2$, and λ_1 and λ_2 are arbitrary constants. The subscripts x and t denote partial derivatives with respect to x and t , respectively. Equation (2) is obtained from the consistency condition $\Psi_{xt} = \Psi_{tx}$ and by substituting $q(x, t) = r^*(x, t) = \psi(x, t)$.

This linear system of 8 equations, Eqs. (3) and (4), reduces to an equivalent system of 4 equations with non-trivial solutions by making the following substitutions: $\lambda_1 = -\lambda_2^*$, $\phi_1 = \psi_2^*$, $\psi_1 = -p^2\phi_2^*$. The reduced system can be solved once the so-called *seed* solution $r(x, t) = q^*(x, t)$ is specified. We have also shown in Ref. [19] that the wavefunction $\psi_0(x, t) = A \exp(i\phi_0)$ with $\phi_0 = t(p^2A^2 - (t^2/3 + x))$, where A is a real constant, is an exact solution of Eq. (2), and thus can be taken as the seed solution.

The Darboux transformation can now be applied to the linear system to generate a new solution of Eq. (2) as follows [18]

$$\psi(x, t) = \psi_0(x, t) - \frac{\sqrt{8}}{p}(\lambda_1 + \lambda_1^*)\phi_2\psi_2^*/(p^2|\phi|^2 + |\psi|^2). \quad (5)$$

Substituting for $\psi_0(x, t)$, $\psi_2(x, t)$, and $\phi_2(x, t)$, we obtain the following new exact solutions to Eq. (2): For the repulsive interactions case ($p = \pm i$), the solution is

$$\psi(x, t) = e^{i\phi_0} \left[A \pm i\sqrt{8}\lambda_{1r} \frac{2u_r^+ \cosh \theta - 2iu_i^+ \sinh \theta + (|u^+|^2 + 1) \cos \beta + i(|u^+|^2 - 1) \sin \beta}{(|u^+|^2 - 1) \sinh \theta + 2u_i^+ \sin \beta} \right], \quad (6)$$

and for the attractive interactions case ($p = 1$), the solution is

$$\psi(x, t) = e^{i\phi_0} \left[A - \sqrt{8}\lambda_{1r} \times \frac{2u_r^+ \cosh \theta - 2iu_i^+ \sinh \theta + (|u^+|^2 + 1) \cos \beta + i(|u^+|^2 - 1) \sin \beta}{(|u^+|^2 + 1) \cosh \theta + 2u_r^+ \cos \beta} \right], \quad (7)$$

where $\theta = \sqrt{2} [\Delta_r(t^2 + x) + 2(\Delta_r\lambda_{1i} - \Delta_i\lambda_{1r})t] - \delta_r$, $\beta = -\sqrt{2} [\Delta_i(t^2 + x) + 2(\Delta_i\lambda_{1i} + \Delta_r\lambda_{1r})t] + \delta_i$, $u^\pm = \sqrt{8}pA/b^\pm$, $b^\pm = 4\lambda_1^* \pm \Delta$, $\Delta = \sqrt{2\lambda_1^{*2} - p^2A^2}$, and δ is an arbitrary constant. Here, the subscripts r and i denote real and imaginary parts, respectively.

Properties of the Solutions.— Here, we describe the main properties and features of the exact solitonic solutions found above. The five arbitrary constants δ_r , δ_i , λ_{1i} , λ_{1r} and A , have the following effects on the solutions: The constants δ_r and δ_i have the trivial effect of shifting the solutions in the x - and t -coordinates. Therefore, we set from now on $\delta_r = \delta_i = 0$. The other three

constants are combined under a square root in the above expression for Δ . Thus, depending on the values of these constants, Δ can be real, imaginary, or complex. If Δ is real, β will have no x -dependence and the solutions will be nonoscillatory, i.e., single-soliton solution. If Δ is imaginary, θ will have no x -dependence, and the solution is oscillatory. If Δ is complex, the solution will be a combination of both previous cases, namely oscillatory but with a localized envelope which has a density profile that is similar to that of *gap* solitons (See Fig.1 of Ref. [21]). These cases are shown in In Table 1, and specific cases are visualized in Fig. 1, where we plot the density $\rho(x, t) = |\psi(x, t)|^2$ at $t = 0$ for the attractive

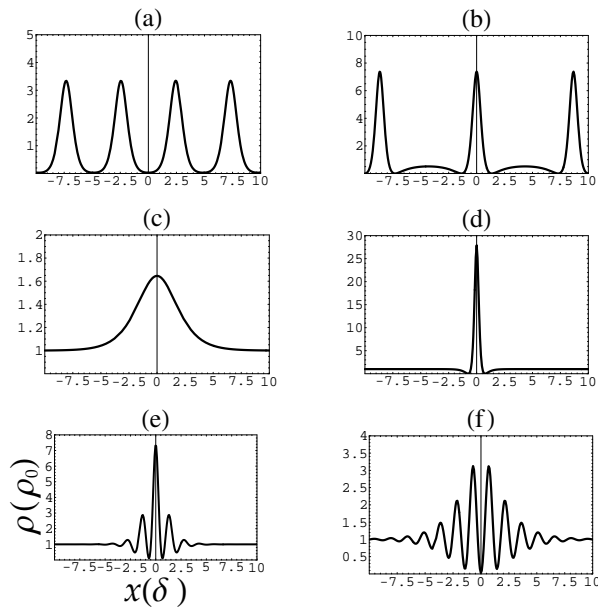


FIG. 1: Density $\rho(x) = |\psi(x)|^2$ at time $t = 0$ for the case of attractive interactions. The arbitrary constants chosen to generate these plots are: $\delta_r = \delta_i = 0$ and $A = 1$ for all plots. In (a) $\lambda_{1i} = 0$, $\lambda_{1r} = 0.29$, in (b): $\lambda_{1i} = 0$, $\lambda_{1r} = -0.6$, in (c): $\lambda_{1i} = 0$, $\lambda_{1r} = 0.8$, in (d): $\lambda_{1i} = 0$, $\lambda_{1r} = -1.5$, in (e): $\lambda_{1i} = 2$, $\lambda_{1r} = -0.6$, and in (f): $\lambda_{1i} = 2$, $\lambda_{1r} = 0.29$. Typical values of the length and density units, δ and ρ_0 , are given in the text.

	$\lambda_{1r} > 0$	$\lambda_{1r} < 0$
$\lambda_{1i} = 0$	multi-solitonic with broad edges	multi-solitonic with sharp edges
$\lambda_{1i} < 0$	single-solitonic with broad edges	single-solitonic with sharp edges
$\lambda_{1i} > 0$	multi-solitonic with envelope	multi-solitonic with envelope

TABLE I: Classification of the solitonic solutions. Fig.1a shows an example of the multi-solitonic solutions with broad edges, Fig.1b shows an example of the multi-solitonic solutions with sharp edges, Fig.1c shows an example of the single-solitonic solutions with broad edges, Fig.1d shows an example of the single-solitonic solutions with sharp edges, and Fig.1d and 1e show an example of the multi-solitonic solutions with an envelope.

interactions case.

For the special choice $\lambda_{1i} = \infty$, the coefficient $u^+ = 0$, and the solutions, Eqs. (6) and (7), reduce to the simple forms:

$$\psi(x, t) = e^{i\phi_0} \left(A \pm i\sqrt{8}\lambda_{1r} e^{-i\beta} \text{csch}\theta \right), \quad (8)$$

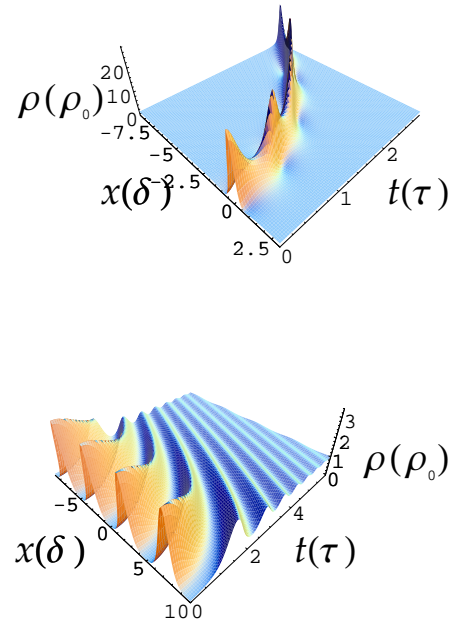


FIG. 2: Color online Surface plots of the density $\rho(x, t) = |\psi(x, t)|^2$ versus x and t for the attractive interactions. The upper plot corresponds to Fig. 1(d) while the lower figure corresponds to Fig 1(a).

$$\psi(x, t) = e^{i\phi_0} \left(A - \sqrt{8}\lambda_{1r} e^{-i\beta} \text{sech}\theta \right). \quad (9)$$

These two equations show that our solution consists of a bright soliton embedded in the background [12].

The trajectory of a given soliton peak is obtained from the condition $\theta = 0$ (for single solitons) or $\beta = 0$ (for multiple solitons). The former gives $x = -t^2 - 2(\lambda_{1i} - \lambda_{1r}\Delta_i/\Delta_r)t + \delta_r/\sqrt{2}$ and the latter gives $x = -t^2 - 2(\lambda_{1i} + \lambda_{1r}\Delta_r/\Delta_i)t + \delta_i/\sqrt{2}$. The trajectory is thus parabolic in time with an acceleration of -1. In real units, this acceleration equals $-F/m$ which is equal to the acceleration associated with the gravity-like waves propagating on the surface of the condensate [23, 24]. This behavior can be clearly seen in Fig. 2.

Using the above relation between x and t , we can eliminate x from ρ to obtain the peak soliton density as a function of time, i.e., along the trajectory. This is shown in Fig. 3 where we notice that the soliton peak oscillates between a minimum and a maximum. The frequency of the oscillation equals $\sqrt{8}|\Delta|^2\lambda_{1r}/\Delta_r$. For the case of Fig. 1(c), where $u_r^+ > 0$, the maximum appears at times defined by $\beta = (2n+1)\pi$, namely $t = n\pi\Delta_r/\sqrt{8}|\Delta|^2\lambda_{1r}$, and the minimum appears at times defined by $\beta = 2n\pi$, $n = 0, 1, 2, \dots$. The maximum peak density is given by $(A + \sqrt{8}\lambda_{1r})^2$ and the minimum peak density is given

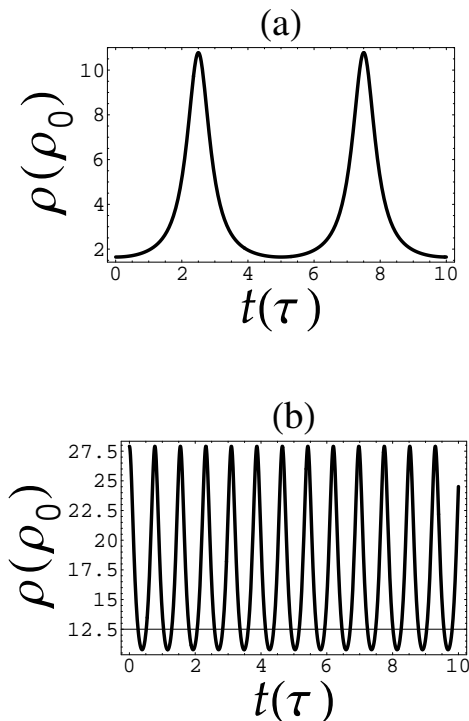


FIG. 3: The soliton peak density along its trajectory for attractive interactions. The upper figure corresponds to Fig. 1(c) and the lower figure corresponds to Fig. 1(d).

by $(A - \sqrt{8}\lambda_{1r})^2$. For the case of Fig. 1(d), the situation is reversed since $u_r^+ < 0$. During this peak oscillation, the number of atoms in the solitons is being exchanged with the background maintaining a dynamic stability [12]. The frequency of atoms exchange is constant with time, unlike the case of Ref. [12].

An interesting feature of the soliton is its phase. We plot in Fig. 4 the phase of a multiple-soliton solution. This shows that the phase difference between the main neighbouring solitons is π . It shows also that this phase difference, the width of solitons, and the distances between them do not change with time. The soliton trains realized experimentally in a one-dimensional condensate with attractive interactions [5] are very similar to our solitonic solutions in Fig. 1(d) and (e). It should be noted here that this is the case since, in addition to describing the surface of the condensate, Eq. 2 describes also a one-dimensional condensate as long as the density is not too large [25]. The center of mass motion of the soliton train in our case is different than in the experiment of [5] due to the fact that we use a linear potential while in the experiment a quadratic potential is used. On the other hand, the density profile, relative phase, and number of solitons in the train can, in principle, be accounted for. This is the case since, in our theory and in the experiment, the width of the individual solitons (of order δ) is

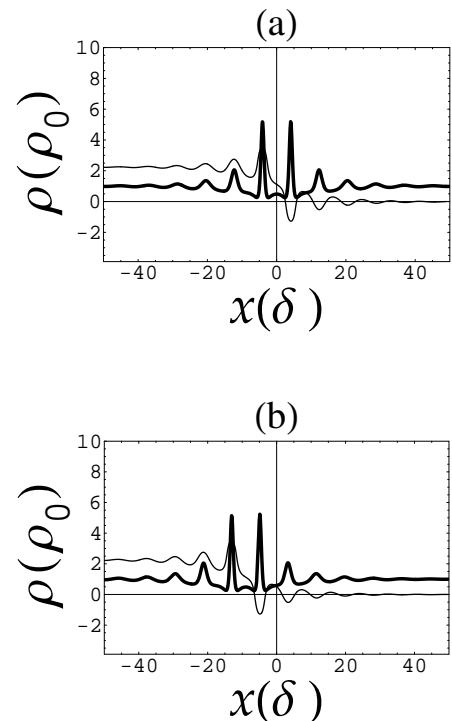


FIG. 4: The density (solid curve) and phase (light curve) of a solitonic solution for attractive interactions with $\delta_r = \delta_i = 0$, $A = 1$, $\lambda_{1i} = 0.03$, and $\lambda_{1r} = 0.6$. The upper plot is for $t = 0$ and the lower plot is for $t = 0.85\tau$.

much less than the that of the background (of order R).

Since the density profile of the exact solitonic solutions found here depend only on the coordinate perpendicular to the surface of the condensate, we predict that in a spherical condensate, a three-dimensional shell-like soliton may exist which in a sense similar to the ones reported in Refs. [26, 28]. Furthermore, the above-described dynamics indicates that, starting from the surface, this shell will be shrinking in radius.

For the case of repulsive interactions, Eq. 6 shows that the density diverges at certain points along the parabolic trajectory described above. These points correspond to the points in Fig 3 where the soliton peak density is maximum. The fact that the density diverges, does not make this solution nonphysical, since the number of atoms in the soliton is finite.

It should be mentioned that exact solitonic solutions of Eq. (2) have been essentially obtained using the so-called inverse-scattering method [27]. However, the present work represents another method of obtaining such exact solitonic solutions. We believe that our method in [19] of obtaining the Lax pair is more systematic since the Lax pair of Ref. [27] was introduced as an assumption. Furthermore, in Ref. [27], only formal solutions are derived for the soliton train case. This is in contrast with the

present work where we obtain explicit single as well as multiple solitons solutions. Finally, while in Ref. [27], only the attractive interactions case is considered, we have derived here solutions for both the attractive and repulsive cases.

In conclusion, we have found exact solitonic solutions of a time-dependent Gross-Pitaevskii equation with linear trapping potential for both cases of attractive and repulsive interatomic interactions. These solutions may be regarded as solitons in the surface region of a three-dimensional Bose-Einstein condensate, or solitons in a one-dimensional condensate.

-
- [1] S. Burger, K. Bongs, S. Dettmer, W. Ertmer, and K. Sengstock, Phys. Rev. Lett. **83**, 5198 (1999).
 - [2] J. Denschlag *et al.*, Science **287**, 97 (2000).
 - [3] B.P. Anderson, P.C. Haljan, C.A. Regal, D.L. Feder, L.A. Collins, C.W. Clark, and E.A. Cornell, Phys. Rev. Lett. **86**, 2926 (2001).
 - [4] L. Khaykovich *et al.*, Science **296**, 1290 (2002).
 - [5] K.E. Strecker, G.B. Partridge, A.G. Truscott, and R.G. Hulet, Nature **417**, 150 (2002).
 - [6] B. Eiermann *et al.*, Phys. Rev. Lett. **92**, 230401 (2004).
 - [7] U. Al Khawaja, *et al.*, Phys. Rev. Lett., **89**, 200404 (2004).
 - [8] L. D. Carr and J. Brand, Phys. Rev. Lett., **92**, 040401 (2004).
 - [9] L.D. Carr and Y. Castin, Phys. Rev. **66**, 063602 (2002).
 - [10] Wu-Ming Liu, B. Wu, and Q. Niu, Phys. Rev. Lett. **84**, 2294 (2000).
 - [11] J. Ieda, T. Miyakawa, and M. Wadati Phys. Rev. Lett. **93**, 194102 (2004).
 - [12] Z.X. Liang, Z.D. Zhang, and W.M. Liu, Phys. Rev. Lett. **94**, 050402 (2005).
 - [13] Lu Li, Zaidong Li, B.A. Malomed, D. Mihalache, and W.M. Liu Phys. Rev. A **72**, 033611 (2005).
 - [14] R. Atre, P.K. Panigrahi, and G.S. Agarwal, Phys. Rev. E **73**, 056611(2006).
 - [15] Th. Busch and J.R. Anglin, Phys. Rev. Lett. **84**, 2298 (2000); L. Salasnich, Phys. Rev. A **70**, 053617 (2004).
 - [16] F. K. Abdullaev, A. Gammal, A. Kamchatnov, L. Tomio, Int. Jour. of Mod. Phys. B, **19**, 3415 (2005).
 - [17] L. Salasnich, A. Parola, and L. Reatto, Phys. Rev. Lett. **91**, 080405 (2003); K. Kasamatsu and M. Tsubota, *ibid.* **93**, 100402 (2004).
 - [18] V.B. Matveev and M.A. Salle, *Dardoux Transformations and Solitons*, Springer Series in nonlinear Dynamics (Springer-Verlag, Berlin, 1991).
 - [19] U. Al Khawaja, to appear in J. Phys. A. (Math. and General) (2006).
 - [20] U. Al Khawaja, *Ph.D. Thesis*, (Copenhagen: Copenhagen University, 1999).
 - [21] B.J. Dabrowska, E.A. Ostrovskaya, and Y.S. Kivshar, J. Opt. B: Quantum Semiclass. Opt. **6**, 423 (2004).
 - [22] E. Lundh, C. J. Pethick, and H. Smith, Phys. Rev. A **55**, 2126 (1997).
 - [23] U. Al Khawaja, C. J. Pethick, and H. Smith, Phys. Rev. A **60**, 1507 (1999).
 - [24] Onofrio *et al.*, Rev. Lett. **84**, 810 (2000).
 - [25] V.A. Brazhnyi and V.V. Konotop, Mod. Phys. Lett. B **18**, 627(2004).
 - [26] D. Mihalache *et al.*, Phys. Rev. A **72**, 021601(R)(2005).
 - [27] H. Chen and C. Liu, Phys. Rev. Lett. **37**, 693 (1976).
 - [28] B.B. Baizakov, B.A. Malomed, and M. Salerno, Europhys. Lett. **63**, 642, (2003).